PHYSICAL REVIEW C VOLUME 21, NUMBER 5 MAY 1980

Actinide muonic atom lifetimes deduced from muon-induced fission

W. W. Wilcke, M. W. Johnson, W. U. Schröder, D. Hilscher, J. R. Birkelund, and J. R. Huizenga
Departments of Physics and Chemistry and Nuclear Structure Research Laboratory, University of Rochester, Rochester, New York 14627

J. C. Browne and D. G. Perry
Los Alamos Scientific Laboratory, Los Alamos, New Mexico 87544
(Received 20 November 1979)

Time distributions of fragments from delayed fission after muon capture have been measured for muonic ^{235}U, ^{238}U, ^{237}Np, ^{239}Pu, and ^{242}Pu. Comparison of these data with previously measured lifetimes using muon decay electrons, neutrons, and γ rays emitted after muon capture indicates that the observed systematic discrepancies are due to atomic muon capture by fission fragments after prompt fission induced by radiationless muonic transitions. The deduced capture rates are compared with theoretical models, and very good agreement is found with a giant-resonance excitation model.

[RADIOACTIVITY Muonic atoms ^{235}U, ^{238}U, ^{237}Np, ^{239}Pu, and ^{242}Pu. Measured fission fragment time distributions, deduced total muon-capture rates and isotopic effect, present data compared to lifetimes based on all other decay channels.]

I. INTRODUCTION

The interaction of negative muons with actinide nuclei has been studied by numerous experiments[1-12] in recent years. These heavy muonic atoms are of particular interest because theories on muon-capture rates, which have been applied successfully for lighter nuclei, can be tested more stringently with very neutron-rich, heavy nuclei.

Experiments designed to determine the capture rate usually measure the time difference between the arrival of a muon in the target and the appearance of any reaction product associated with the capture of the muon by the nucleus. Since muon capture excites a heavy nucleus on the average to approximately 15 MeV, various reaction products including neutrons, fission fragments, and γ rays can be observed. In addition, it is possible to infer the muon-capture rate from the time distribution of electrons emitted in the leptonic decay of muons in the 1s state of a muonic atom. It was generally assumed that all these methods yield the same lifetimes for a particular muonic atom, but it soon became obvious that lifetimes measured by detecting fission fragments emitted after muon capture were consistently slightly shorter than lifetimes determined with any other method. Hadermann[13] pointed out the likely cause of this discrepancy: It is well known that "prompt fission" may occur during the atomic cascade of a muon to its ground state due to a radiationless transfer of the muonic transition energy to the nucleus. In the course of such a prompt fission process, the muon may become bound in an atomic orbital of one of the fission fragments and may later be captured by the fragment or undergo leptonic decay. In a singles experiment as described above, electrons, neutrons, and γ rays resulting from muonic fission fragments cannot be distinguished from those stemming from muon capture by the actinide nuclei. Hence, the time distributions of electrons, neutrons, and γ rays consist of a superposition of two exponential components. The characteristic lifetimes are 70–80 nsec for muonic actinides and about 130 nsec[14,15] for heavy muonic fission fragments. The capture of muons by the light fission fragment does occur only with low probability.[14,15] However, the statistics of most experiments is not sufficient to allow a distinction of the various components of the measured time distributions such that least-square fits assuming a simple exponential decay law for these distributions will yield lifetimes that are too long.

In contrast, because muon capture by a fission fragment cannot induce fission of this fragment, time distributions of delayed fission fragments produced by muon capture are not disturbed by prompt fission events. There are, however, two secondary effects that lead to insignificant contamination of these time distributions: The radiationless atomic transition of a muon can cause the emission of one neutron from the target nucleus before subsequent fission of the daughter nucleus occurs after muon capture. This process has a probability similar to prompt fission, but since the lifetime difference between two neighboring isotopes is only about 1.5 nsec for actinide nuclei (as estimated from a study[11] of ^{235,238}U and ^{239,242}Pu), the effect of this admixture on the lifetimes deduced is more than one order of magnitude smaller

© 1980 The American Physical Society

than the effect of prompt fission on measurements of electrons, neutrons, and γ rays described above, and is well within the statistical uncertainties of all experiments performed so far. The second mechanism that may affect the time distribution of fission fragments is the possible excitation of shape-isomeric nuclear states during the muonic cascade, as suggested by Bloom.[16] A quantitative discussion[11] shows, however, that the influence of this effect on the measured lifetime is very small.

Muon capture by fission fragments as proposed by Hadermann[13] and delayed fission after prompt neutron emission, however, have been observed directly in coincidence experiments, where the emission of fission fragments in coincidence with decay electrons[14] and neutrons[15] was measured. In addition, a measurement[11] with very good statistics confirmed the presence of a long-lifetime component in the singles time spectrum of neutrons emitted from muonic ^{239}Pu. Therefore, it is concluded that measurements employing the experimentally rather unambiguous fission technique are required to provide meaningful data on muon-capture rates for actinides that can be compared to theoretical models of muon capture. Coincidence experiments would be even better, but their statistical accuracy is inherently lower than that of singles measurements. Since the effects of prompt neutron emission and isomeric-state excitation on fission time distributions are negligible, the present study of singles fission measurements was initiated with the aim of obtaining data of high statistical accuracy.

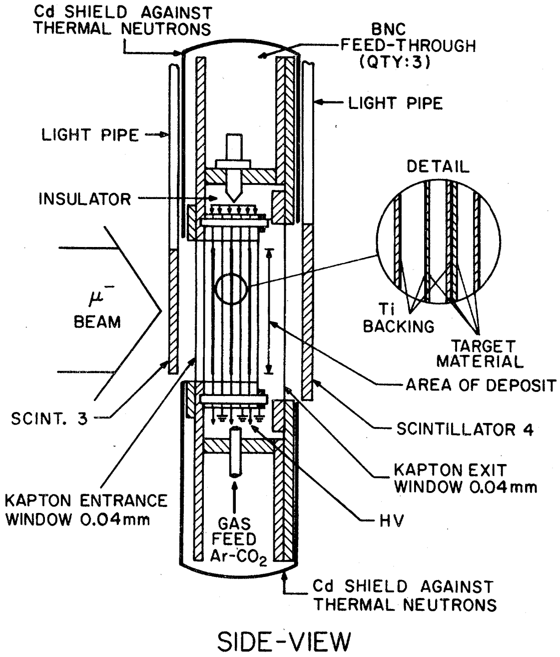

FIG. 1. Schematic drawing of the fission ionization chamber. The insert shows the arrangement of the target foils used to avoid cross talk between different sets of foils: The foil on the left is part of the adjacent electrically decoupled chamber which uses the same gas volume.

II. EXPERIMENTAL PROCEDURE

The experiments were performed using the stopped-muon channel of the Los Alamos Meson Physics Facility (LAMPF). Muons from the channel passed through a three-element plastic scintillator telescope and were stopped in a fission chamber containing nine Ti foils, on which the actinide targets (^{235,238}U, ^{237}Np, and ^{239,242}Pu) were deposited as 0.5 mg/cm^2 thick oxide layers. Since inspection of previous experiments[1-12] indicated that systematical errors are frequently more important than statistical ones, care was taken to minimize the former by measuring three isotopes simultaneously. As shown in Fig. 1, three foils carrying one particular isotope formed an ionization chamber, and three such chambers constituted the whole fission chamber. All timing signals were processed in the same time-to-pulse-height converter and the same analog-to-digital converter (ADC), using routing signals to distinguish the ionization chamber that had fired. Time calibrations were performed frequently with several independent methods. In addition, only two isotopes were replaced at a time, so that the third isotope remaining in the chamber served as an additional

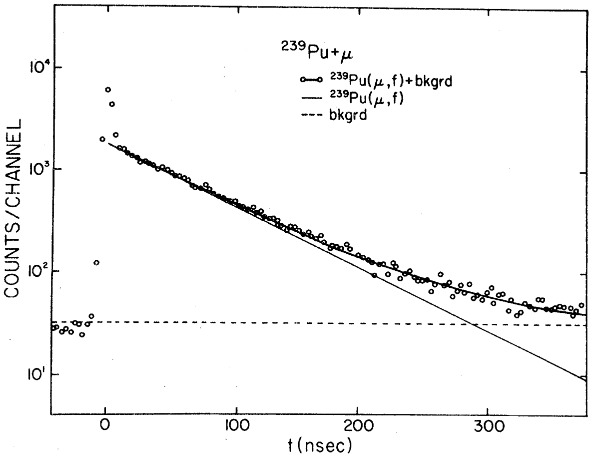

FIG. 2. The experimental fission-fragment time distribution for muonic ^{239}Pu. The peak in the region near $t = 0$ corresponds to prompt fission events caused by radiationless muonic transitions. The horizontal dashed line represents a fit to the background to negative and large positive times. The curve drawn through the data points represents the sum of the exponential and the background distributions.

cross check for the consistency of the results for different runs. A typical time spectrum is shown in Fig. 2. The data were analyzed with a least-squares code and a fitting function representing an exponential distribution on a constant background. A trial fit assuming two exponentials failed to find a second lifetime component in the spectra, as was to be expected.

III. EXPERIMENTAL RESULTS AND DISCUSSION

The experimental results are compiled in Table I along with all previously published data on muonic actinide lifetimes τ_i. The indices e, n, γ, and f refer to electron-, neutron-, γ-ray-, and fission fragment measurements, respectively. The weighted averages $\bar{\tau} \pm \sigma$ have been calculated[17] by weighting the data τ_i according to the published error $\tau_i \pm \sigma_i$ using the following equations:

$$\bar{\tau} = \frac{\sum(\tau_i/\sigma_i^2)}{\sum(1/\sigma_i^2)}, \tag{1}$$

$$\sigma_A = \left[\frac{\sum(\tau_i - \bar{\tau})^2/\sigma_i^2}{(n-1)\sum(1/\sigma_i^2)}\right]^{1/2}, \tag{2}$$

$$\sigma_B = \left[\sum(1/\sigma_i^2)\right]^{-1/2}, \tag{3}$$

$$\sigma = \max(\sigma_A, \sigma_B). \tag{4}$$

Equation (2) for the error σ_A of the weighted mean can yield unphysical values for very small samples. Therefore, σ_B was introduced which sets a lower limit for σ based on the published errors. Inspection of Table I shows that for all isotopes the averaged lifetime $\bar{\tau}_f$ is shorter than either τ_n, $\bar{\tau}_\gamma$, or $\bar{\tau}_e$.

Although there is no question about the occurrence of muon capture by fission fragments, it has not been shown that this mechanism is the only one responsible for the differences between measured lifetimes. A systematical study of all muonic actinides may be helpful to shed light on this question, since a monotonic increase of the (positive) difference $\tau_n - \bar{\tau}_f$ is expected with increasing probability for prompt fission, if muon capture by fission fragments were the dominant contribution to these differences. It is possible to define a characteristic parameter allowing a systematic classification of muonic actinides. Such a suitable parameter is represented by the product of the proba-

TABLE I. Experimental lifetimes in nsec of muonic actinides deduced from measurements of decay electrons (τ_e), neutrons (τ_n), capture γ rays (τ_γ), and fission fragments (τ_f). As discussed in the text, the electron, neutron, and γ-ray lifetime measurements yield values systematically too high, because these three measurements are sensitive to contributions from muon capture by fission fragments after prompt fission. The lifetimes τ_f deduced from a detection of delayed fission fragments, however, are not affected by this effect. The weighted average $\bar{\tau}_f$ of the fission lifetimes is therefore believed to represent the best values for the true muonic actinide lifetimes.

Isotope	τ_e	$\bar{\tau}_e$	τ_n	τ_γ	τ_f	$\bar{\tau}_f$
^{232}Th	80.4 ± 2.0[2] 79.2 ± 2.0[3]	79.8 ± 1.4	80.1 ± 0.6[11]		74.2 ± 5.6[5] 87.0 ± 4.0[6] 77.3 ± 0.3[12]	77.4 ± 0.5
^{233}U					61.7 ± 3.8[4]	61.7 ± 3.8
^{235}U	78 ± 4[2] 75.4 ± 1.9[3]	75.9 ± 1.7	75.0 ± 0.7[11]		65.3 ± 2.8[4] 66.5 ± 4.2[5] 75.6 ± 2.3[6] 72.9 ± 0.9[a]	72.6 ± 1.5
^{238}U	88 ± 4[1] 81.5 ± 2.0[2] 73.5 ± 2.0[3]	78.7 ± 3.5	78.3 ± 1.0[11]	78.6 ± 1.5[9] 79.1 ± 0.5[10] $\bar{\tau}_\gamma$: 79.0 ± 0.5	74.1 ± 2.8[4] 75.6 ± 2.9[5] 76.0 ± 1.0[6] 77.1 ± 0.2[12] 77.9 ± 0.5[a]	77.2 ± 0.2
^{237}Np			73.5 ± 1.4[11]		72 ± 2[8] 71.3 ± 0.9[a]	71.4 ± 0.8
^{239}Pu	77.5 ± 2.0[2] 73.4 ± 2.8[3]	76.1 ± 1.9	74.5 ± 0.5[11]		74 ± 14[7] 70 ± 3[8] 70.1 ± 0.7[a]	70.1 ± 0.7
^{242}Pu			81.1 ± 0.7[11]		79 ± 5[8] 75.4 ± 0.9[a]	75.5 ± 0.9

[a] Present study.

bility of a radiationless muonic transition and the fissility of the target nucleus. As has been shown by Zaretski and Novikov,[18] the ratio of radiationless to radiative transition probabilities is given approximately by

$$\frac{\Gamma_{rl}}{\Gamma_r} \approx Z\alpha , \tag{5}$$

where $\alpha = e^2/\hbar c$ is the fine-structure constant. The probability of fission after a radiationless transition depends in a complicated way on the detailed shape of the double-humped fission barrier, which is augmented in the presence of the muon. It is assumed, however, that the general trend of the fissility be still given by the liquid-drop expression for the fissility[19] $X \sim Z^2/A$. Combining X with Eq. (5), one obtains a suitable scale $p(Z,A)$ for discussing the lifetimes:

$$p = X\frac{\Gamma_{rl}}{\Gamma_{rl}+\Gamma_r} = \frac{\alpha Z^3}{50.13A(1+Z\alpha)} . \tag{6}$$

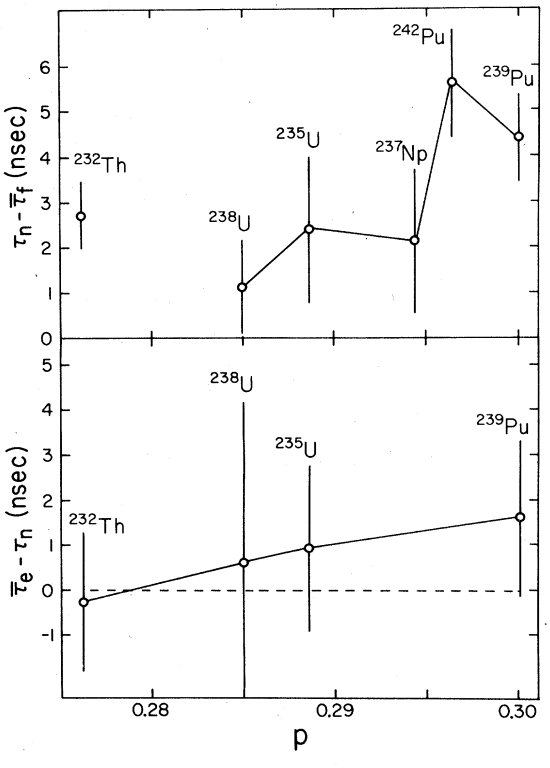

FIG. 3. The upper part shows the difference $\tau_n - \bar{\tau}_f$ of the lifetimes measured by detecting neutrons and fission fragments, respectively, after muon capture, plotted versus the product p of liquid-drop fissility and probability for radiationless transitions. Large values of this quantity, which is an approximate measure for the prompt fission probability, are correlated with large lifetime differences. The lower part shows the lifetime difference $\bar{\tau}_e - \tau_n$ between results of experiments detecting electrons and neutrons, respectively. Since $\bar{\tau}_e$ is more sensitive to contributions from muonic fission fragments than τ_n, this difference is also weakly correlated with p.

In the upper part of Fig. 3 the difference $\tau_n - \bar{\tau}_f$ of lifetimes is plotted versus p. Except for ^{232}Th, the difference $\tau_n - \bar{\tau}_f$ is seen to increase with increasing values of p as expected, if muon capture by fission fragments were the dominant cause of the lifetime differences. It is known,[8] however, that the prompt fission probability of muonic ^{242}Pu is very large, even larger than that for ^{239}Pu. Hence, the high value of $\tau_n - \bar{\tau}_f$ for ^{242}Pu is understandable, but the result for ^{232}Th is puzzling. It is known[6] that ^{232}Th has a very low probability (5×10^{-4}) for prompt fission, which is consistent with its low p value. Therefore, muon capture after prompt fission cannot explain the large difference of the lifetimes. It should be pointed out, however, that the weighted average of $\bar{\tau}_f$ for ^{232}Th is dominated by one measurement.[12] More data are needed to firmly establish the abnormal behavior for ^{232}Th shown in Fig. 3(a).

As has been discussed in the introduction, both electron and neutron measurements are influenced by the occurrence of prompt fission, whence the difference of lifetimes $\bar{\tau}_e - \tau_n$ should be small. This difference may be nonzero, however, since the two methods are of different sensitivity to the admixture of events resulting from muon capture by a fission fragment: The multiplicity M_n of neutrons emitted after muon capture in a β-stable nucleus of mass A is approximately given[20] by

$$M_n \approx 0.3A^{1/3} . \tag{7}$$

In addition, the muon-capture rate decreases rapidly with decreasing atomic mass, whereas the muon decay rate remains essentially constant. Thus the ratio of electron-to-neutron multiplicity is about twice as high for heavy muonic fission fragments as compared to muonic actinides. Therefore, the difference $\bar{\tau}_e - \tau_n$ should increase slightly with p, consistent with experimental results shown in the lower part of Fig. 3. With the possible exception of ^{232}Th, the systematic comparison of the data indicates that muon capture by fission fragments is the dominant contribution to the differences in lifetime. Therefore, $\bar{\tau}_f$ represents the best approximation to the true lifetime of a muonic actinide.

The experimental results may be compared to existing theories for muon-capture rates λ that are related to the measured lifetimes $\bar{\tau}_f$ by

$$\frac{1}{\bar{\tau}_f} = \lambda^{\exp} + R\lambda_0 . \tag{8}$$

Here λ_0 is the free-muon decay rate, and R (~0.85) accounts for the reduction of the decay rate due to effects of atomic binding.[3] Two theoretical approaches have been applied to the study of muon-capture rates in the actinide region. The well-known Goulard-Primakoff formalism[21] has been proved useful in predicting muon-capture rates over a wide range[22] of isotopes and provides a closed-form equation for the total muon-capture rate λ^{GP}:

$$\lambda^{GP} = kZ_{\text{eff}}^4\left(1-\frac{\epsilon_\mu}{m_\mu}\right)^2\left(1-\frac{m_\mu\epsilon_\mu}{m_N}\right) \times\left[1-0.03\frac{A}{2Z}+0.25\frac{A-2Z}{2Z} -3.24\left(\frac{A-Z}{2A}+\frac{|A-2Z|}{8ZA}\right)\right]. \tag{9}$$

The notation is that of Ref. 11. A comparison of the Goulard-Primakoff predictions to the experimentally observed capture rates is given in Table II. The predicted rates are systematically smaller than the measured ones. The Goulard-Primakoff capture rates are proportional to the value of Z_{eff}^4, which has to be calculated independently, but a comparison of several isotopes of the same element, which nearly eliminates the dependence on Z_{eff}^4, indicates that this theory consistently overrates the sensitivity of the capture rate to the neutron excess. In the alternate model[23] of Kozłowski and Zgliński the capture mechanism proceeds solely via the excitation of giant-resonance states. The transition amplitude M_V is given by the overlap integral of Pustovalov's muon wave function[24] and the neutrino wave function within the nuclear volume with an isovector transition operator and nuclear wave functions taken from the hydrodynamical model.[25] Multipolarities L from monopole to octupole are taken into account, and the total muon-capture rate λ^{KZ} is the sum of the rates for each multipolarity:

$$\lambda^{KZ} = \frac{m_\mu^2}{2\pi}G_\mu^2\sum_{L=0}^{3}|(M_V)_L|^2. \tag{10}$$

TABLE II. Comparison of experimentally determined muon-capture rates $\lambda^{\exp}$ with the predictions of the Goulard-Primakoff (λ^{GP}) and Kozłowski-Zgliński (λ^{KZ}) theories. Units are 10^5 sec^{-1}.

Isotope	$\lambda^{\exp}$	λ^{GP}	λ^{KZ}
^{232}Th	125 ± 1	110	124
^{233}U	158 ± 9	131	
^{235}U	134 ± 1	122	134
^{238}U	125 ± 1	108	122
^{237}Np	137 ± 1	123	138
^{239}Pu	139 ± 2	129	139
^{242}Pu	129 ± 2	116	128

This model has been applied[26] to the nuclei under investigation (Table II), and the agreement between theory and experiment is excellent. It has been shown[27] that for light nuclei (e.g. ^{16}O) the giant resonances are very effective doorway states for muon capture. In heavy nuclei, however, numerous noncollective states at 15–20 MeV excitation energy are expected to exist, which also fulfill the spin and isospin selection rules of the operators describing muon capture. Therefore, it is rather surprising that a model which incorporates only giant-resonance states describes the capture rates so well. It appears important to check other consequences of the proposed capture mechanisms by experiment. Measurements of the neutron multiplicity and energy spectra after muon capture in actinides currently under way will yield information on the excitation energy spectrum and can be compared to this model.

ACKNOWLEDGMENTS

This work was supported by the U.S. Department of Energy. We would like to thank the technical staff of the Los Alamos Meson Physics Facility and especially L.E. Agnew and B.R. Rector for their hospitality and assistance, and J.G. Povelites for preparing the targets.

---

[1] J. C. Sens, Phys. Rev. 113, 679 (1959).

[2] O. Hashimoto, S. Nagamiya, K. Nagamine, and T. Yamazaki, Phys. Lett. 62B, 233 (1976).

[3] M. W. Johnson, W. U. Schröder, J. R. Huizenga, W. K. Hensley, D. G. Perry, and J. C. Browne, Phys. Rev. C 15, 2169 (1977).

[4] B. Budick, S. C. Cheng, E. R. Macagno, A. M. Rushton, and C. S. Wu, Phys. Rev. Lett. 24, 604 (1970).

[5] J. A. Diaz, S. N. Kaplan, and P. V. Pyle, Nucl. Phys. 40, 54 (1963).

[6] D. Chultem, V. Cojocaru, Dz. Ganzorig, Kim Si Chwan, T. Krogulski, V. C. Kuznetsov, H. G. Ortlepp, S. M. Polikanov, B. M. Sabirov, V. Schmidt, and W. Wagner, Nucl. Phys. A247, 452 (1975).

[7] V. Cojocaru, L. Marinescu, M. Petrascu, G. Vioculescu, A. Ignatenko, and M. Omelianenko, Phys. Lett. 20, 53 (1966).

[8] B. M. Aleksandrov, G. V. Buklanov, W. D. Fromm, Dz. Ganzorig, A. S. Krivokhatski, T. Krogulski, S. M. Polikanov, and B. M. Sabirov, Phys. Lett. 57B, 238 (1975).

[9] W. D. Fromm, H. G. Ortlepp, S. M. Polikanov, U. Schmidt, G. N. Zorin, R. Arlt, and G. Musiol, Nucl. Phys. A278, 387 (1977).

[10] S. N. Kaplan, J. A. Monard, and S. Nagamiya, Phys. Lett. 64B, 217 (1976).

[11] W. W. Wilcke, M. W. Johnson, W. U. Schröder, J. R. Huizenga, and D. G. Perry, Phys. Rev. C 18, 1452 (1978).

[12] Dz. Ganzorig, P. G. Hansen, T. Johansson, B. Jonson, J. Konijn, T. Krogulski, V. D. Kuznetsov, S. M. Polikanov, G. Tibell, and L. Westgaard, Phys. Lett. 78B, 41 (1978).

[13] J. Hadermann, Phys. Lett. 67B, 35 (1977).

[14] Dz. Ganzorig, P. G. Hansen, T. Johansson, B. Jonson, J. Konijn, T. Krogulski, V. D. Kuznetsov, S. M. Polikanov, G. Tibell, and L. Westgaard, Phys. Lett. 77B, 257 (1978).

[15] W. U. Schröder, W. W. Wilcke, M. W. Johnson, D. Hilscher, J. R. Huizenga, J. C. Browne, and D. G. Perry, Phys. Rev. Lett. 43, 672 (1978).

[16] S. D. Bloom, Phys. Lett. 48B, 470 (1974).

[17] P. R. Bevington, *Data Reduction and Error Analysis for the Physical Sciences* (McGraw-Hill, New York, 1969), Chap. 5.

[18] D. F. Zaretsky and V. M. Novikov, Nucl. Phys. 28, 177 (1961).

[19] R. Vandenbosch and J. R. Huizenga, *Nuclear Fission* (Academic, New York, 1973), Chap. 2.

[20] P. Singer, *Springer Tracts in Modern Physics* (Springer, Berlin, 1974), Vol. 71, p. 39.

[21] B. Goulard and H. Primakoff, Phys. Rev. C 10, 2034 (1974).

[22] M. Eckhause, R. T. Siegel, R. T. Welsh, and T. A. Fillippas, Nucl. Phys. 81, 525 (1966). The Primakoff fit performed in this study corresponds to a theory preceding Ref. 21 as described in H. Primakoff, Rev. Mod. Phys. 31, 802 (1959).

[23] T. Kozłowski and A. Zgliński, Nucl. Phys. A305, 368 (1978).

[24] G. E. Pustovalov, Zh. Eksp. Teor. Fiz. 36, 1288 (1959) [Sov. Phys.—JETP 36, 1806 (1959)].

[25] A. Bohr and B. R. Mottelson, *Nuclear Structure* (Benjamin, New York, 1975), Vol. 2.

[26] A. Zgliński and T. Kozłowski, private communication.

[27] J. D. Walecka, *Muon Physics*, edited by V. W. Hughes and C. S. Wu (Academic, New York, 1975), Vol. 2.